Prognostic phenotypes of early-stage lung adenocarcinoma

Anne-Sophie Lamort[1,2,9], Jan Christian Kaiser[3,9], Mario A.A. Pepe[1,2], Ioannis Lilis[4], Giannoula Ntaliarda[4], Kalman Somogyi[2,5], Magda Spella[4], Sabine J. Behrend[1,2], Georgia A. Giotopoulou[1,2], Willem Kujawa[1,2], Michael Lindner[2,6], Ina Koch[2,6], Rudolf A. Hatz[2,6], Juergen Behr[2,7], Rocio Sotillo[2,5,8], Andrea C. Schamberger[1,2] and Georgios T. Stathopoulos[1,2,9]

[1]Comprehensive Pneumology Center (CPC) and Institute for Lung Biology and Disease (iLBD), Helmholtz Center Munich–German Research Center for Environmental Health (HMGU), Munich, Germany. [2]German Center for Lung Research, Giessen, Germany. [3]Institute of Radiation Medicine (IRM), Helmholtz Center Munich–German Research Center for Environmental Health (HMGU), Neuherberg, Germany. [4]Dept of Physiology, Faculty of Medicine, University of Patras, Rio, Greece. [5]Division of Molecular Thoracic Oncology, German Cancer Research Center (DKFZ), Heidelberg, Germany. [6]Center for Thoracic Surgery Munich, Ludwig Maximilian University of Munich and Asklepios Medical Center, Gauting, Germany. [7]Dept of Medicine V, University Hospital, Ludwig Maximilian University of Munich, Munich, Germany. [8]Translational Lung Research Center Heidelberg (TRLC), German Center for Lung Research (DZL), Heidelberg, Germany. [9]These authors contributed equally to this work.

Corresponding author: Georgios T. Stathopoulos (stathopoulos@helmholtz-muenchen.de)

Shareable abstract (@ERSpublications)
Clinical-grade immunodetection of TP53, NF1, CD45, PD-1, PCNA, TUNEL and FVIII in tumour samples identifies two phenotypes of resected lung adenocarcinomas that display different prognosis and can be used for patient management and trial design https://bit.ly/3DpM5Ll

Cite this article as: Lamort A-S, Kaiser JC, Pepe MAA, *et al*. Prognostic phenotypes of early-stage lung adenocarcinoma. *Eur Respir J* 2022; 60: 2101674 [DOI: 10.1183/13993003.01674-2021].

This article has an editorial commentary: https://doi.org/10.1183/13993003.00569-2022

Received: 14 June 2021
Accepted: 11 Nov 2021

Abstract

Background Survival after curative resection of early-stage lung adenocarcinoma (LUAD) varies and prognostic biomarkers are urgently needed.

Methods Large-format tissue samples from a prospective cohort of 200 patients with resected LUAD were immunophenotyped for cancer hallmarks TP53, NF1, CD45, PD-1, PCNA, TUNEL and FVIII, and were followed for a median of 2.34 (95% CI 1.71–3.49) years.

Results Unsupervised hierarchical clustering revealed two patient subgroups with similar clinicopathological features and genotype, but with markedly different survival: "proliferative" patients (60%) with elevated TP53, NF1, CD45 and PCNA expression had 50% 5-year overall survival, while "apoptotic" patients (40%) with high TUNEL had 70% 5-year survival (hazard ratio 2.23, 95% CI 1.33–3.80; p=0.0069). Cox regression and machine learning algorithms including random forests built clinically useful models: a score to predict overall survival and a formula and nomogram to predict tumour phenotype. The distinct LUAD phenotypes were validated in The Cancer Genome Atlas and KMplotter data, and showed prognostic power supplementary to International Association for the Study of Lung Cancer tumour–node–metastasis stage and World Health Organization histologic classification.

Conclusions Two molecular subtypes of LUAD exist and their identification provides important prognostic information.

Introduction

Lung adenocarcinoma (LUAD), the most frequent histologic subtype of lung cancer, accounts for an estimated 1 million annual deaths [1, 2]. Although surgical resection remains the preferred definitive cure for early-stage LUAD [3], survival thereafter is highly variable, necessitating the development and validation of prognostic biomarkers [4]. Such biomarkers can be clinicopathological features [5–7], genomic alterations [8–12], gene expression profiles [13, 14], imaging characteristics [15, 16] and immunohistochemical expression of single markers [17–22]. However, no biomarker to date has found widespread applicability. Patients with resectable LUAD are currently treated with (neo)adjuvant chemotherapy, radiotherapy, targeted therapy and/or immunotherapy dictated by tumour–node–metastasis (TNM) stage and driver mutations, and are followed in a uniform fashion [3, 9–12]. This is in contrast to other cancer types, where immunodetection of key tumour hallmarks dictates therapy and prognosis. For

example, immunohistochemistry (IHC) expression of marker of proliferation Ki-67 and oestrogen, progesterone and epidermal growth factor type 2 receptors dictate treatment and prognosis in breast cancer [23].

Here, we analysed 200 patients with resected LUAD [7] using conventional (non-tissue microarray-based) IHC of large, representative tumour tissue areas and a clinical-grade scoring system for cancer hallmarks [24] tumour protein 53 (TP53), neurofibromatosis 1 (NF1), cluster of differentiation 45 (CD45), programmed cell death-1 (PD-1), proliferating cell nuclear antigen (PCNA), terminal deoxynucleotidyl nick-end labelling (TUNEL) and anti-haemophilic factor (FVIII). We followed patients for prolonged periods of time (cumulative/median follow-up 507/2.34 (95% CI 1.71–3.49) years) to discover two phenotypes of LUAD with markedly different overall survival. These phenotypes were validated in two independent datasets. Clinicians are provided with tools to predict LUAD phenotype and with proposals for their potential clinical implementation.

Materials and methods

Research resources are listed using Research Resource Identifiers (RRIDs) (https://scicrunch.org/resources) and CAS Registry Numbers (www.cas.org/cas-data/cas-registry), where appropriate.

Study design

The present study was conducted in accordance with the Helsinki Declaration, was prospectively approved by the Ludwig Maximilian University of Munich Ethics Committee (623-15) and was registered at the German Clinical Trials Register (DRKS00012649). All patients gave written informed consent.

During 2011–2017, 200 patients with full clinical data and ample available tissues were recruited for the present study, designed to reflect the whole cohort of 366 patients [7] (supplementary table E1) and to detect medium effect sizes (d=0.25) with α=0.05 and β=0.90 using G*Power academic software (www.psychologie.hhu.de/arbeitsgruppen/allgemeine-psychologie-und-arbeitspsychologie/gpower; RRID:SCR_013726).

Patient data and tumour samples

Anonymised data and samples were comprehensively reviewed by a dedicated panel (A-S.L., J.C.K., M.A. A.P., S.J.B., G.A.G., A.C.S., M.L., I.K., R.A.H., J.B. and G.T.S.), including International Association for the Study of Lung Cancer (IASLC) TNM stage (the 7th edition (TNM7) was used due to the timing of the study) [25], World Health Organization (WHO) histologic growth pattern (the 2015 classification was used) [2, 5] and "spread through air spaces" (STAS) [26–28]. Tissue samples were cut into two equal parts for IHC and for DNA/RNA extraction using guanidinium thiocyanate–phenol–chloroform extraction (TRIzol; Thermo Fisher, Waltham, MA, USA).

IHC and TUNEL

Tissues were formalin-fixed (CAS 50-00-0) and paraffin-embedded (CAS 8002-74-2), cut into serial tissue sections (5 µm thick), and stained with primary antibodies and their corresponding horseradish peroxidase-linked secondary antibodies (supplementary table E2). For negative controls, primary antibodies were omitted. TUNEL was performed with the Click-iT TUNEL kit (Thermo Fisher). For negative controls, dUTP (CAS 94736-09) was omitted. Slides were counterstained with haematoxylin (Roth, Karlsruhe, Germany; CAS 517-28-2) and coverslipped using Entellan (Merck, Darmstadt, Germany). 10 different areas of each tumour and five different fields of view of each tissue section were analysed by three trained blinded readers (A-S.L., W.K. and G.T.S.) at low magnification (×20), the percentage of stained cells was semiquantitatively scored as 0 (<5%), 1 (5–24%), 2 (25–49%), 3 (50–74%) or 4 (>74%) on an Eclipse E400 microscope (Nikon, Melville, NY, USA; RRID:SCR_020320) using TCapture software (Tucsen Photonics, Fuzhou, China; RRID:SCR_020956) and the results were averaged by patient, as routinely done and described elsewhere [17–20, 23]. Cancer-specific hallmark expression was also determined in randomly selected paired normal lung tissues (n=50).

Digital droplet PCR

DNA was purified with GenElute Mammalian Genomic DNA Miniprep (Sigma-Aldrich, St Louis, MO, USA), and *KRAS* codon 12/13 and *EGFR* exon 19 were analysed with digital droplet PCR *KRAS* G12/G13 and *EGFR* exon 19 del Screening Kits, respectively, using QuantaSoft Analysis Pro software (Bio-Rad, Hercules, CA, USA). Data were normalised by accepted droplet numbers to yield absolute mutation allelic frequencies; 25% mutant droplets was used as the cut-off to discriminate wild-type from mutant tumours.

ALK *fusion detection*

50 ng RNA was used for reverse transcription using the Quantitect Reverse Transcription Kit (Qiagen, Hilden, Germany). The manufacturer's protocol was followed, except that 0.25 µL *ALK*-specific reverse

primer (hAlk.cdna.rev1) was added to the primer mix to enrich transcripts carrying the 3′ part of the *ALK* gene. RNA from human cell lines (NCI-H3122, *EML4/ALK* variant 1, RRID:CVCL_5160; NCI-H2228, *EML4/ALK* variant 3, RRID:CVCL_1543) served as positive controls. 10 µL PCR reactions were performed using HotStarTaq Master Mix (Qiagen) and 200 ng cDNA template. PCR products were run on 10% agarose gels. *EML4-ALK*-positive reactions were repeated, and the PCR products were purified and sequenced to confirm *EML4/ALK* transcripts. Variant-specific forward (hEml4.cdna.v1.for1; hEml4.cDNA.v2.for1; hEml4.cdna.v3.for1) and universal reverse (hAlk.cdna.rev2) primer sequences were: hAlk.cdna.rev1, CTCCTTCAGGTCACTGATGG; hAlk.cdna.rev2, TTGCCAGCAAAGCAGTAGTTGG; hEml4.cdna.v1.for1, AGTTTCACCCAACAGATGCAAATACC; hEml4.cdna.v2.for1, TAGATGAACCAGGACACTGTGCAG; hEml4.cdna.v3.for1, AGCCCTCTTCACAACCTCTCC.

Computational analyses and statistics

Statistics and heatmap visualisations were done using R* (www.r-project.org; RRID:SCR_001905) and Prism version 8.0 (GraphPad, San Diego, CA, USA; RRID:SCR_002798). Unsupervised hierarchical clustering was performed using Euclidean distance and clustering method “ward.D2” on the R* package pheatmap (RRID:SCR_016418). To investigate predictors of overall survival and prevalence of the proliferative phenotype, a combination of machine learning and regression techniques was applied. Kaplan–Meier, Cox regression and random forests were selected to determine optimal cut-offs and overall survival at different end-points (1 and 3 years). Random forests were grown using the R* package randomforestSRC (RRID:SCR_015718). Covariables for further regression analysis were confirmed based on mean decreased accuracy. From simulated random forests, nonparametric estimates of probabilities for overall survival depending on pertinent covariables (TP53, NF1, CD45, PD-1, PCNA, TUNEL and FVIII) were derived. Partial probability estimates were generated by focusing on a single covariable of interest for which the influence of the remaining covariables was averaged out by summation. Random forest results were used to obtain suggestions for pertinent covariables, to guide the introduction of nonlinear categorical dependencies, and to produce a formula and a nomogram for single-patient phenotype prediction. Overall survival analyses were done with Kaplan–Meier estimates and Cox regression (RRID:SCR_021137). Moreover, survival objects were formed in R* based on right-censored follow-up and survival status which were used in random forest generation and Cox regression. The quality of data explanation for random forests was judged by area under the curve (AUC) in classification mode. However, random forests were mainly applied to guide the regression analysis and not for rigorous prediction assessment. Finally, the preferred regression models were chosen based on goodness-of-fit measured by the Akaike Information Criterion (AIC) and biological plausibility. To characterise the predictive power of a given model, the AUC for logistic regression and the integrated AUC (or concordance) for Cox regression were reported. Associations between variables were examined using Mann–Whitney tests, two-way ANOVA with Šídák’s post-tests, Chi-squared tests, Fischer’s exact tests and Spearman’s correlations. Two-tailed probabilities $p<0.05$ were considered significant. Graphs and tables were generated in Prism version 8.0 and Excel (Microsoft, Redmond, WA, USA).

Results

We selected 200 patients with complete clinical information and ample LUAD and adjacent lung tissues that were representative of the originating cohort (supplementary table E1) [7]. All 200 large-format tumour samples as well as 50 randomly selected normal tumour-adjacent lung samples were immunolabelled for TP53, NF1, CD45, PD-1, PCNA, TUNEL and FVIII, and 10 independent tumour areas were scored for immunoreactivity on a clinically relevant semiquantitative 0 (none)–4 (highest) scale, using normal lung tissues as background controls. Average relative interobserver variability was <5% for any blinded reader comparison and the three scores for each sample/marker were averaged. Raw data are given in supplementary figure E1 and supplementary table E3.

All seven cancer hallmarks were overexpressed in tumour compared with adjacent lung tissues (figure 1). Unsupervised hierarchical clustering of IHC data alone using Euclidean metrics identified two patient clusters: a majority cluster highly expressing the intercorrelated markers TP53, NF1, CD45 and PCNA comprised of 121 (60%) patients (hereafter called “proliferative”) and a minority highly TUNEL-labelled cluster encompassing 79 (40%) patients (hereafter called “apoptotic”) (figure 2a and b, and supplementary figure E2). Interestingly, cancer hallmark IHC and the two patient clusters were only marginally or not at all correlated with clinicopathological variables (including sex, smoking status, chronic obstructive pulmonary disease stage, histologic growth pattern, STAS, pathologic TNM7 stage and oncogene status), likely reflecting something novel (figure 2b and c, and supplementary figures E3 and E4). Importantly, proliferative compared with apoptotic patients displayed markedly decreased overall survival (5-year survival 50% *versus* 70%, respectively; hazard ratio (HR) 2.23, 95% CI 1.33–3.80; log-rank p=0.0069), while STAS and mutation status had no impact on overall survival (figure 2d). To validate the existence of

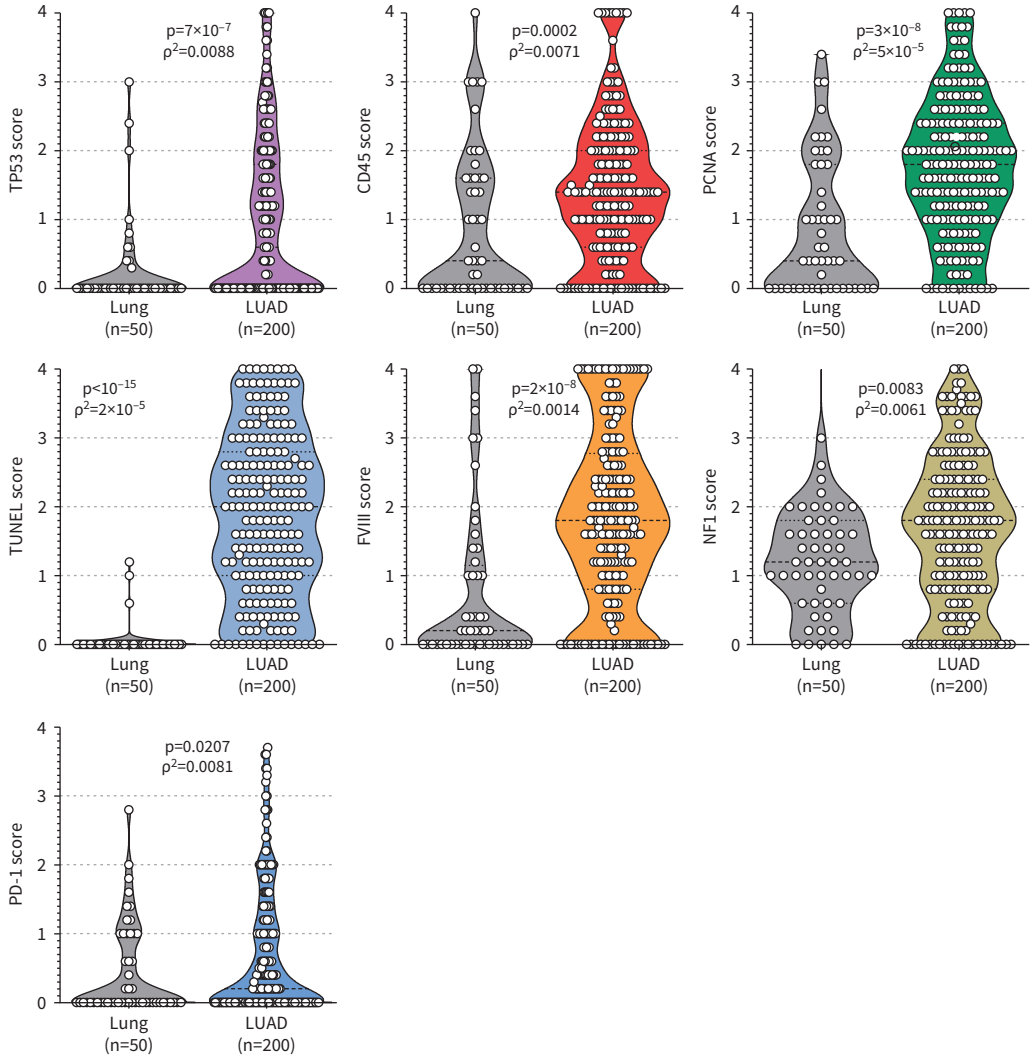

FIGURE 1 Immunophenotyping of early-stage lung adenocarcinoma (LUAD) (n=200) and randomly selected adjacent normal lung tissues (n=50) for seven cancer hallmarks. Data are shown as raw data points (circles) on a semiquantitative scale from 0 (no expression) to 4 (highest expression), rotated kernel density distributions (violins), medians (dashed lines), quartiles (dotted lines), patient numbers (n), p-values (Mann–Whitney test) and squared Spearman's correlation coefficients (ρ^2) for n=50 tumour–normal tissue pairs. Note that all seven cancer hallmarks are overexpressed in cancerous compared with adjacent tissues and that expression values between the two compartments are not correlated. TP53: tumour protein 53; CD45: cluster of differentiation 45; PCNA: proliferating cell nuclear antigen; TUNEL: terminal deoxynucleotidyl transferase dUTP nick-end labelling; FVIII: coagulation factor VIII; NF1: neurofibromatosis 1; PD-1: programmed cell death protein 1.

these two molecular LUAD phenotypes, we analysed The Cancer Genome Atlas LUAD pan-cancer data (https://bit.ly/3blzgFp), which include reverse-phase protein assay data for TP53 and PCNA (but none of the other markers) from 340 patients [29]. Similar to our findings, TP53 and PCNA protein expression were tightly correlated, unsupervised hierarchical clustering identified two patient clusters with high (n=134 (39%)) and low (n=206 (61%)) TP53/PCNA expression ratios, and patients with a high PCNA/TP53 expression ratio displayed significantly worse overall survival (figure 3). Collectively, these results suggest the existence of two LUAD phenotypes, *i.e.* proliferative and apoptotic, in two independent patient cohorts (figure 4a).

We next analysed the impact of individual cancer hallmarks on overall survival using univariate Kaplan–Meier estimates of our cohort stratified by optimal cut-offs defined by the KMplotter custom module (http://kmplot.com/analysis/index.php?p=service&cancer=custom_plot), performed multivariate Cox

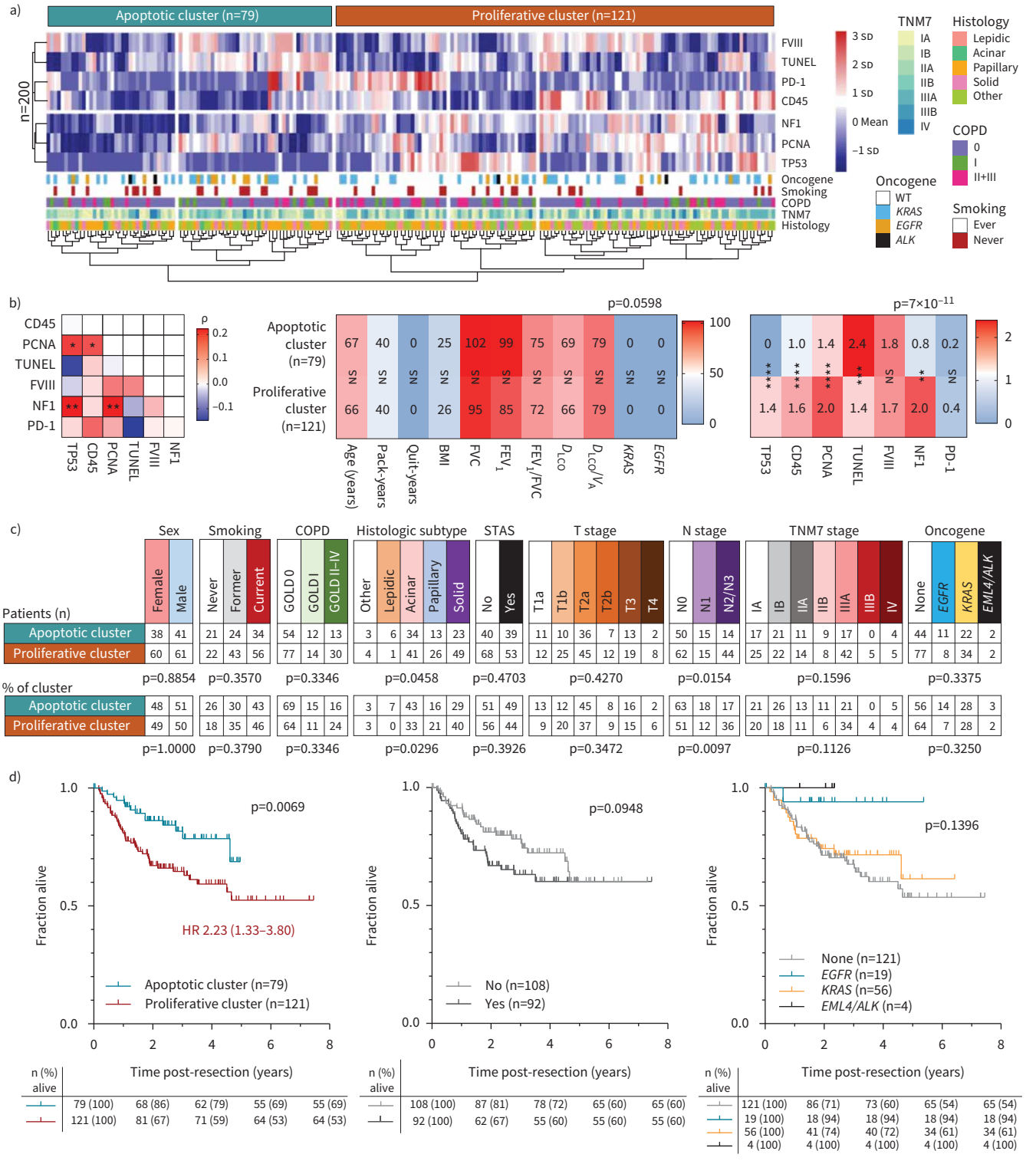

FIGURE 2 Two patient clusters of early-stage lung adenocarcinoma (LUAD) with markedly different survival. a) Heatmap shows unsupervised hierarchical clustering of n=200 patients by immunohistochemistry of tumour tissues for seven cancer hallmarks. Each column represents one patient and each row represents one marker. b) Heatmaps show Spearman's correlation coefficients (ρ) between immunoreactivity for the seven markers (left), as well as median parametric clinical variables (middle) and median marker expression (right) for proliferative and apoptotic patient clusters. Data are shown as ρ (left) and median values (middle and right), patient numbers (n), and p-values (two-way ANOVA). Left: *: p<0.05; **: p<0.01, Spearman's correlation. Middle and right: NS: nonsignificant (p>0.05); **: p<0.01; ***: p<0.001; ****: p<0.0001, for comparison between the two clusters (Šídák's post-test). c) Cross-tabulations of proliferative and apoptotic cluster patient numbers (n) and percentages (%) stratified by nonparametric variables, with p-values (Chi-squared test or Fischer's exact test). d) Overall survival of all patients stratified by immunophenotypic

cluster (left), "spread through air spaces" (STAS) (middle) and oncogene status (right). Data are shown as patient numbers (n), Kaplan–Meier survival estimates (lines), censored observations (line marks), survival tables, hazard ratio (95% CI) and log-rank p-values. FVIII: coagulation factor VIII; TUNEL: terminal deoxynucleotidyl transferase dUTP nick-end labelling; PD-1: programmed cell death protein 1; CD45: cluster of differentiation 45; NF1: neurofibromatosis 1; PCNA: proliferating cell nuclear antigen; TP53: tumour protein 53; COPD: chronic obstructive pulmonary disease; TNM: tumour–node–metastasis; WT: wild-type; BMI: body mass index ($kg \cdot m^{-2}$); FVC: forced vital capacity (% pred); FEV_1: forced expiratory volume in 1 s (% pred); D_{LCO}: diffusing capacity of the lung for carbon monoxide (% pred); V_A: alveolar volume (L); GOLD: Global Initiative for Chronic Obstructive Lung Disease.

regression and grew random forests. High TP53 and PCNA expression emerged as significant predictors of worse overall survival by all three methods, while high CD45 expression was associated with worse overall survival on Cox and random forest analyses (figure 4b–e). Importantly, TP53, PCNA and CD45 competed with important clinicopathological predictors of overall survival identified previously in several independent cohorts, such as T and N stage and histologic growth pattern, as well as patient age, lung function and smoking status (figure 4f) [4–7]. In addition to TP53, PCNA and CD45, there was also a trend for the remaining cancer hallmarks to impact overall survival (figure 5a, graphs). These findings show that IHC-assessed expression of stand-alone cancer hallmarks, especially TP53, PCNA and CD45, possesses some weak prognostic power for incipient overall survival of resected LUAD.

To improve the prognostic power of individual cancer hallmarks and to provide clinicians with a tool to manage individual patients, all cancer hallmarks were incorporated in an unweighted immunophenotypic LUAD death score ($LADERS_{IMM}$), in homology to a clinical LUAD death score ($LADERS_{CLIN}$) developed previously [7], according to cut-offs determined by a single method or a combination of methods (figure 5a, table). We designed $LADERS_{IMM}$ for easy clinical implementation on any individual patient, by incorporating high expression of TP53, NF1, CD45, PCNA and FVIII as predictors of worse overall survival and of TUNEL and PD-1 as predictors of better overall survival. Indeed, 66 patients with high $LADERS_{IMM}$ (5–6 points) had 5-year overall survival of 43%, while 118 patients with intermediate $LADERS_{IMM}$ (3–4 points) 61% and 16 patients with low $LADERS_{IMM}$ (0–2 points) 100%, with 2–3-fold hazard ratios for every low-to-intermediate-to-high $LADERS_{IMM}$ increment (figure 5b and c). When $LADERS_{IMM}$ and $LADERS_{CLIN}$ (a survival score that incorporates age, lung function, N stage, time from diagnosis to resection and histologic growth pattern, and that outperforms TNM7 stage in predicting survival) [7] were compared by correlation, linear regression and κ statistic of agreement, they were only weakly related, hence they are positioned to synergise in predicting overall survival (figure 5d). To this end, 73 patients with intermediate or high values (⩾3) for both scores had 25% 5-year overall survival, while the remaining 127 patients had >75% 5-year overall survival, for a >5-fold hazard ratio (figure 5e). These data support the clinical applicability of $LADERS_{IMM}$ alone or in combination with TNM stage and other clinicopathological prognosticators of overall survival in patients with resected LUAD. To validate $LADERS_{IMM}$, mRNA expression data for the seven cancer hallmarks TP53, NF1, CD45, PD-1, PCNA, TUNEL and FVIII were sought in the KMplotter lung cancer module (https://kmplot.com/analysis/index.php?p=service&cancer=lung). When good probes for our markers were not available, the most relevant genes were used (*CLTA* for CD45, *SPATA2* for PD-1, *MKI67* for PCNA and apopain/*CASP3* for TUNEL). Again, all markers independently performed similar to our cohort in predicting better or worse overall survival (figure 6a). When their average expression was examined (apopain/*CASP3* and PD-1 were inverted similar to $LADERS_{IMM}$), the combination of cancer hallmarks equivalent to $LADERS_{IMM}$ predicted overall survival in all lung cancers and in LUAD, but not in squamous cell lung carcinoma (figure 6b). Hence, cancer hallmarks TP53, NF1, CD45, PD-1, PCNA, TUNEL and FVIII alone or combined into a score predict overall survival in two independent LUAD patient cohorts. We further compared $LADERS_{IMM}$ with IASLC TNM7 stage and WHO histologic subtype in predicting overall survival using Kaplan–Meier and Cox analyses. $LADERS_{IMM}$ was inferior to TNM7, but superior to WHO histology (figure 7a–c), and its prognostic power was stronger in patients with advanced TNM7 stage or solid growth pattern known to have poor overall survival [2, 5, 25], indicating its complementarity to the TNM7 and WHO classifications.

As opposed to using individual cancer hallmarks to directly predict overall survival, we next examined whether cancer hallmark IHC can be integrally used to identify individual patient phenotype and to indirectly prognose overall survival. Using logistic regression and random forests, all cancer hallmarks except PD-1 predicted phenotype (figure 8a and b). In figure 8c we provide a formula and its performance measures designed for clinical use to predict LUAD phenotype. The formula for Microsoft Excel is $P_{PROLIFERATIVE}$=1/(1+e^(−(−4.9+2.5*TP53+1.9*CD45+1.2*PCNA−1.1*TUNEL−0.7*FVIII+1.7*NF1))), where cancer hallmark scores range from 0 (none) to 4 (highest). For this, we used cross-validation with the leave-one-out method. Cut-off $P_{PROLIFERATIVE}$=0.538 was determined for maximal specificity/

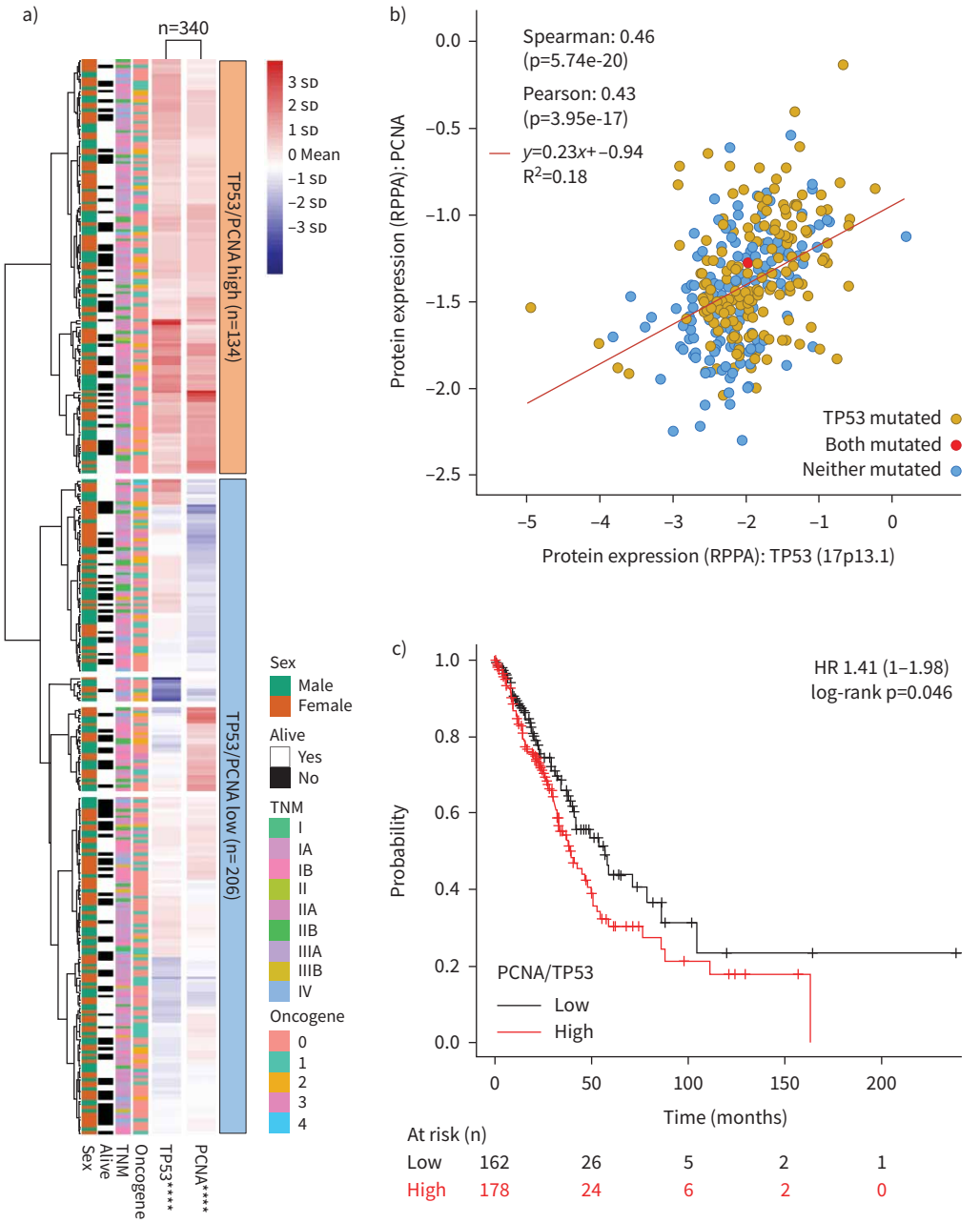

FIGURE 3 The Cancer Genome Atlas (TCGA) protein data support the existence of two lung adenocarcinoma (LUAD) phenotypes. Tumour protein 53 (TP53) and proliferating cell nuclear antigen (PCNA) protein expression (no others from the selected markers are available) in n=340 patients with LUAD from the TCGA pan-cancer dataset define two patient clusters, are tightly correlated and determine overall survival. Data were retrieved from www.cbioportal.org on 19 March 2021. a) Heatmap shows unsupervised hierarchical clustering of n=340 patients by protein expression of tumour tissues for TP53 and PCNA assessed by reverse-phase protein assay (RPPA). Each row represents one patient and each column represents one marker. ****: p<0.0001, for comparison between the two clusters (Šídák's post-test). b) Correlation and linear regression between TP53 and PCNA protein expression. Shown are raw data points (circles) colour-coded by mutation status, Spearman's correlation coefficients and p-values, as well as linear regression line, formula and p-value. c) Overall survival of all patients stratified by PCNA/TP53 expression ratio. Data are shown as patient numbers (n), Kaplan–Meier survival estimates (lines), censored observations (line marks), survival table, hazard ratio (95% CI) and log-rank p-value. Raw data were analysed using the KMplotter custom module on 19 March 2021 (https://kmplot.com/analysis/index.php?p=service&cancer=custom_plot). TNM: tumour–node–metastasis.

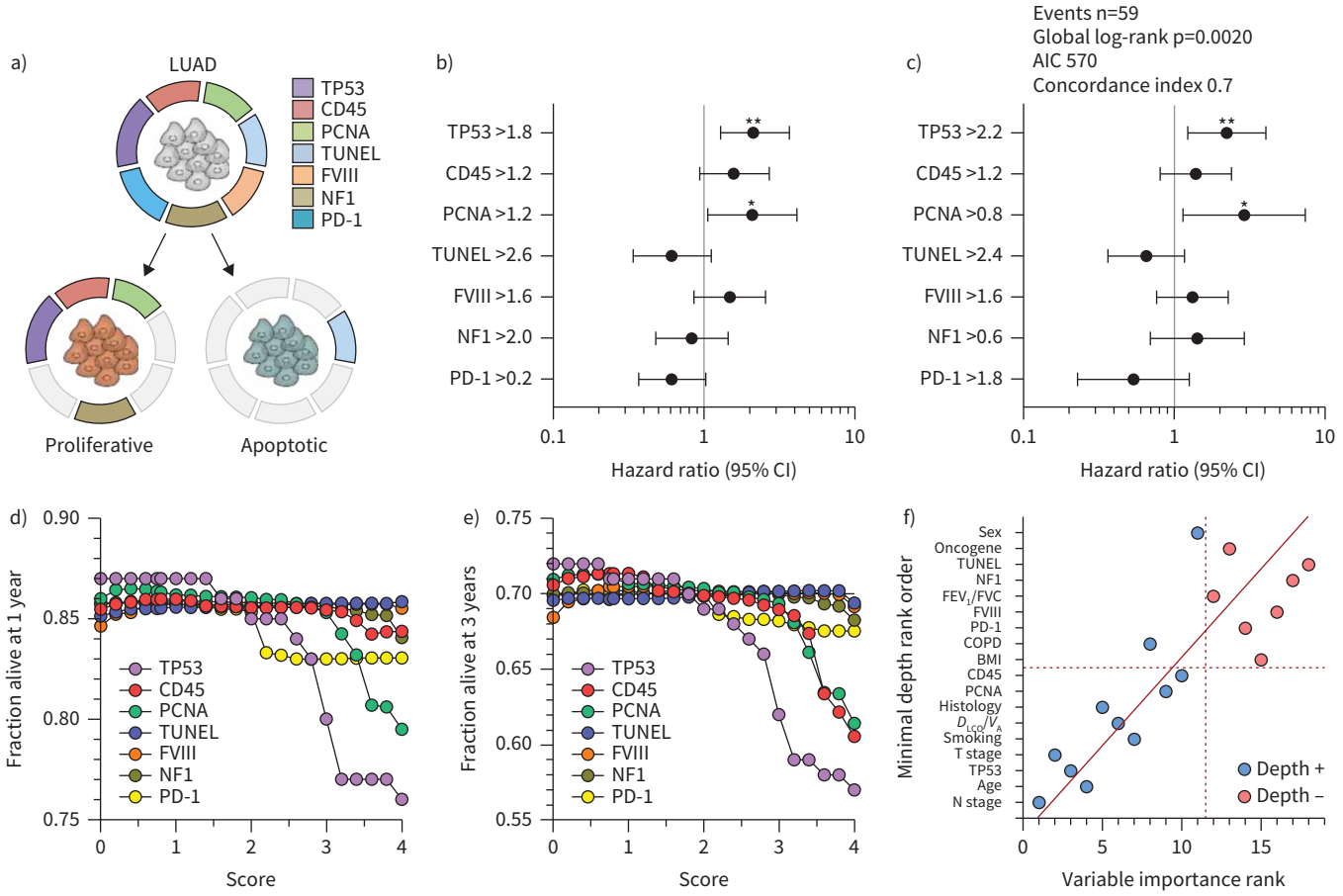

FIGURE 4 Single-marker analyses targeted at overall survival. a) Schematic of the two identified lung adenocarcinoma (LUAD) phenotypes and their respective cancer hallmark expression patterns. b–f) Overall survival analyses by single-marker cut-offs optimised using b) univariate Kaplan–Meier estimates, c) multivariate Cox regression, d, e) random forest analyses with end-points set at d) 1 year and e) 3 years, and f) variable importance plot of variable importance rank from random forest probability values *versus* minimal depth rank order from logistic regression. Data in b, c) are shown as immunoreactivity cut-offs (*y*-axis numbers) and hazard ratios (95% CI). *: p<0.05; **: p<0.01, compared with hazard ratio=1 (log-rank test in b) and Cox regression in c)). Data in d, e) are shown as probability of overall survival by marker expression. Data in f) are shown as estimates (circles), cut-offs (dashed lines) and regression (solid line). TP53: tumour protein 53; CD45: cluster of differentiation 45; PCNA: proliferating cell nuclear antigen; TUNEL: terminal deoxynucleotidyl transferase dUTP nick-end labelling; FVIII: coagulation factor VIII; NF1: neurofibromatosis 1; PD-1: programmed cell death protein 1; AIC: Akaike Information Criterion; FEV_1: forced expiratory volume in 1 s; FVC: forced vital capacity; BMI: body mass index; D_{LCO}: diffusing capacity of the lung for carbon monoxide; V_A: alveolar volume; T: tumour; N: node.

sensitivity as the median of n=200 $P_{OPTIMAL}$ from cross-validation. $P_{PROLIFERATIVE}$>0.538 means classification of a patient as proliferative, whereas $P_{PROLIFERATIVE}$≤0.538 means classification of a patient as apoptotic. The formula is visualised as a nomogram (figure 8d) and is easily applicable (patient examples in supplementary figure E5). The receiver operator characteristic curve of the formula (figure 8e) achieves AUC 96%, while the agreement of the formula and nomogram with actual patient phenotype was almost perfect (κ 0.833, 95% CI 0.755–0.912). Formula/nomogram-predicted phenotype significantly affected overall survival, performing equal to actual phenotype (figure 8f). Hence, cancer hallmarks collectively can determine patient phenotype using a formula or a nomogram, indirectly prognosticating overall survival.

Discussion

Here, we assessed the expression of seven key cancer hallmarks [24] of genomic instability (TP53), KRAS pathway activation (NF1), tumour-associated inflammation (CD45), immune checkpoint activity (PD-1), cellular proliferation (PCNA), tumour cell apoptosis (TUNEL) and angiogenesis (FVIII) in a cohort of patients with early-stage resected LUAD hypothesising that this will aid prognosis. We examined large-format tumour and normal tissues, and applied clinical-grade semiquantitative scoring to multiple

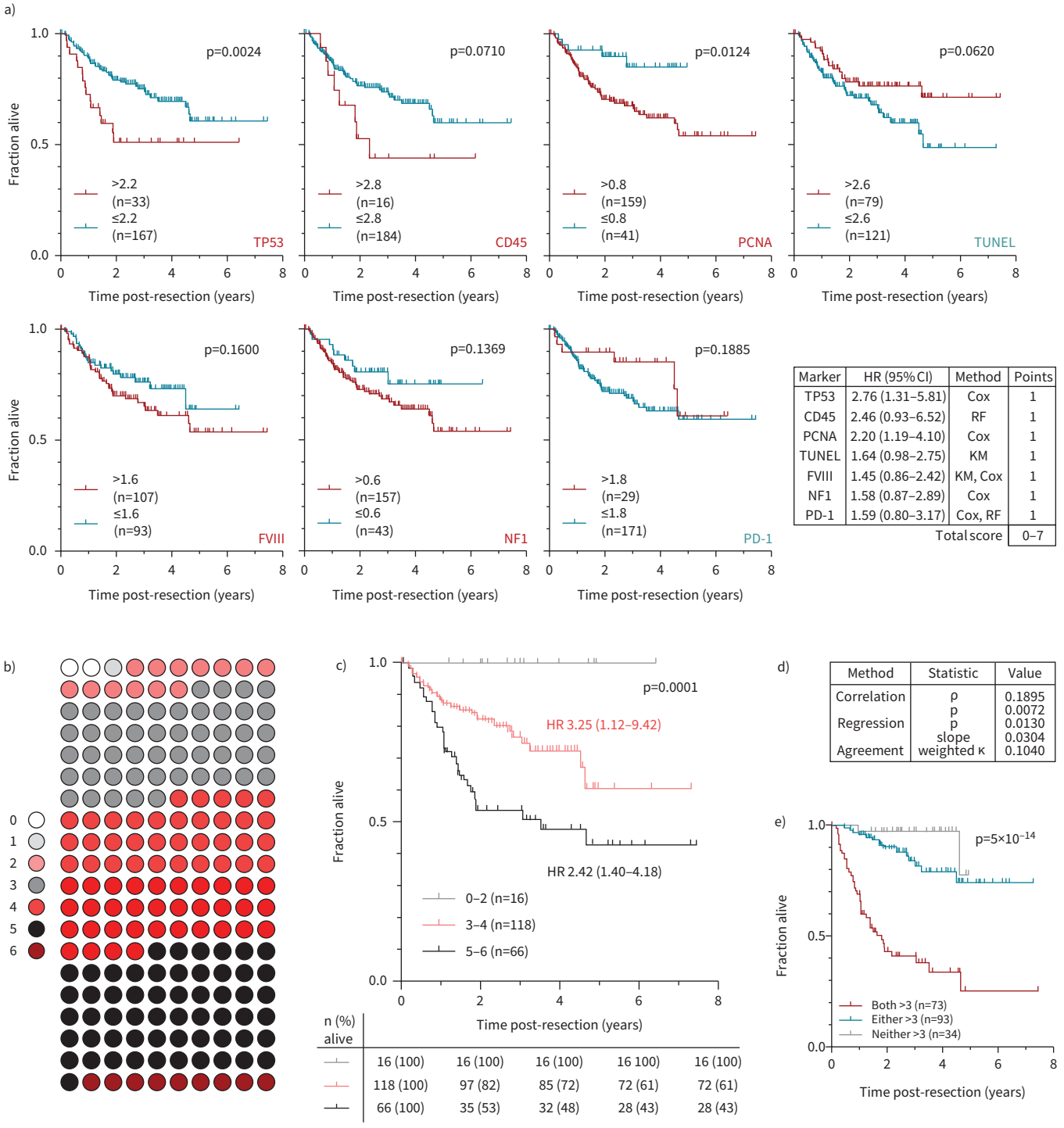

Marker	HR (95% CI)	Method	Points
TP53	2.76 (1.31–5.81)	Cox	1
CD45	2.46 (0.93–6.52)	RF	1
PCNA	2.20 (1.19–4.10)	Cox	1
TUNEL	1.64 (0.98–2.75)	KM	1
FVIII	1.45 (0.86–2.42)	KM, Cox	1
NF1	1.58 (0.87–2.89)	Cox	1
PD-1	1.59 (0.80–3.17)	Cox, RF	1
		Total score	0–7

Method	Statistic	Value
Correlation	ρ	0.1895
	p	0.0072
Regression	p	0.0130
	slope	0.0304
Agreement	weighted κ	0.1040

FIGURE 5 An immunophenotypic score determines survival in lung adenocarcinoma (LUAD). a) Univariate (Kaplan–Meier (KM)), multivariate (Cox) and random forest (RF) survival analyses identified optimised cut-offs of single-marker immunoreactivity. Shown is overall survival of all patients stratified by single-marker immunoreactivity (graphs) and composite immunophenotypic survival score (table). b) Patient distribution by immunophenotypic LUAD death score ($LADERS_{IMM}$). c) Overall survival of all patients stratified by $LADERS_{IMM}$. d) Comparison of $LADERS_{IMM}$ with a previously derived clinical LUAD death score ($LADERS_{CLIN}$) shows that these are only marginally related. Shown are Spearman's correlation coefficient (ρ) and p-value, linear regression p-value and slope, and weighted agreement coefficient (κ). e) Overall survival of all patients stratified by both $LADERS_{IMM}$ and $LADERS_{CLIN}$ [7]. Data in a, c, e) are shown as patient numbers (n), KM survival estimates (lines), censored observations (line marks) and p-values (log-rank test), with or without hazard ratio (95% CI). TP53: tumour protein 53; CD45: cluster of differentiation 45; PCNA: proliferating cell nuclear antigen; TUNEL: terminal deoxynucleotidyl transferase dUTP nick-end labelling; FVIII: coagulation factor VIII; NF1: neurofibromatosis 1; PD-1: programmed cell death protein 1.

https://doi.org/10.1183/13993003.01674-2021

a)

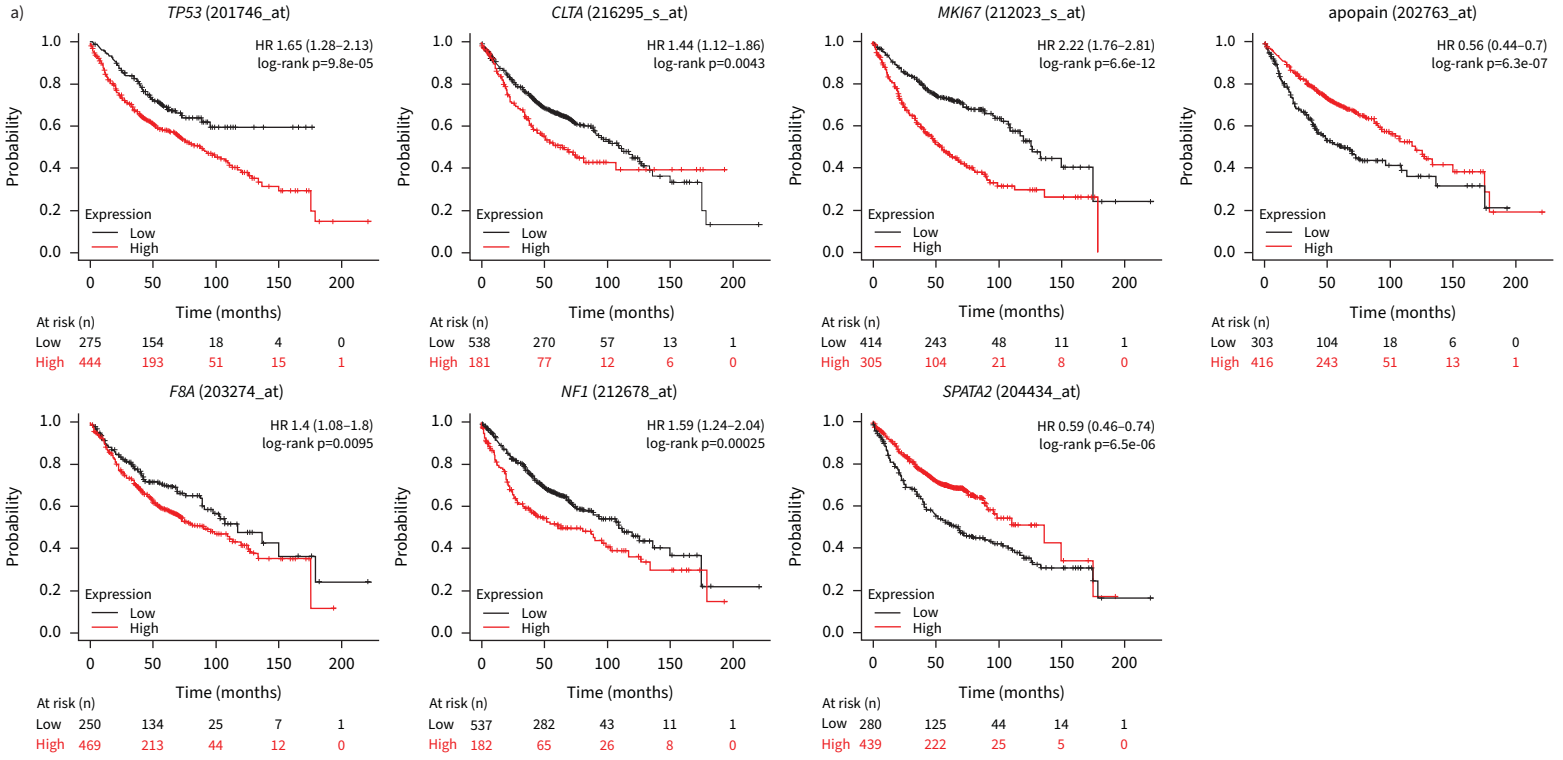

b)

Marker	KMplot RNA	KMplot probe	Weight
TP53	*TP53*	201746	+1
CD45	*CLTA*	216295	+1
PCNA	*MKI67*	212023	+1
TUNEL	*CASP3*	202763	−1
FVIII	*F8A*	203274	+1
NF1	*NF1*	212678	+1
PD-1	*PD1*	204434	−1

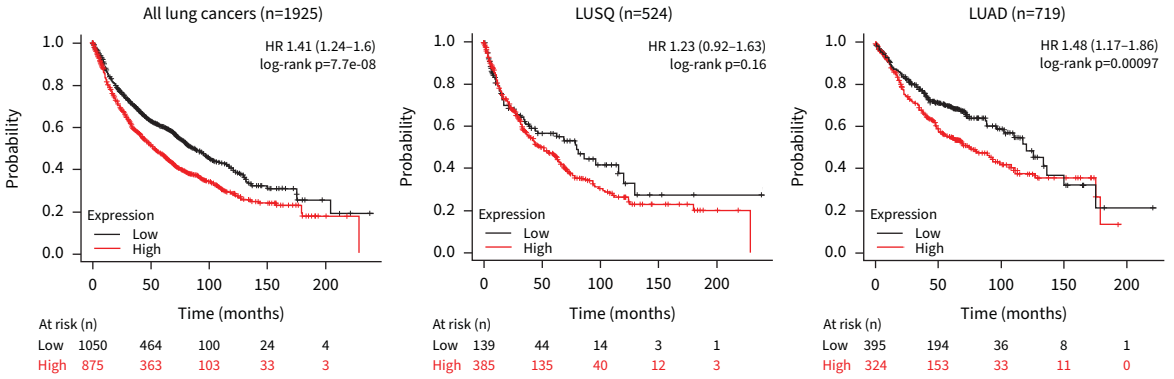

FIGURE 6 A gene expression profile related to immunophenotype determines survival in lung adenocarcinoma (LUAD). Univariate overall survival analyses by optimised cut-offs of a) LUAD patients by single markers and b) all lung cancer patients by median expression of all markers (apopain and *SPATA2* inverted). Data are shown as patient numbers, Kaplan–Meier survival estimates (lines), censored observations (line marks), survival tables, hazard ratios (95% CI) and log-rank p-values. Data were from the KMplotter lung cancer genechip module (https://kmplot.com/analysis/index.php?p=service&cancer=lung). TP53: tumour protein 53; CD45: cluster of differentiation 45; PCNA: proliferating cell nuclear antigen; TUNEL: terminal deoxynucleotidyl transferase dUTP nick-end labelling; FVIII: coagulation factor VIII; NF1: neurofibromatosis 1; PD-1: programmed cell death protein 1; LUSQ: squamous cell lung carcinoma.

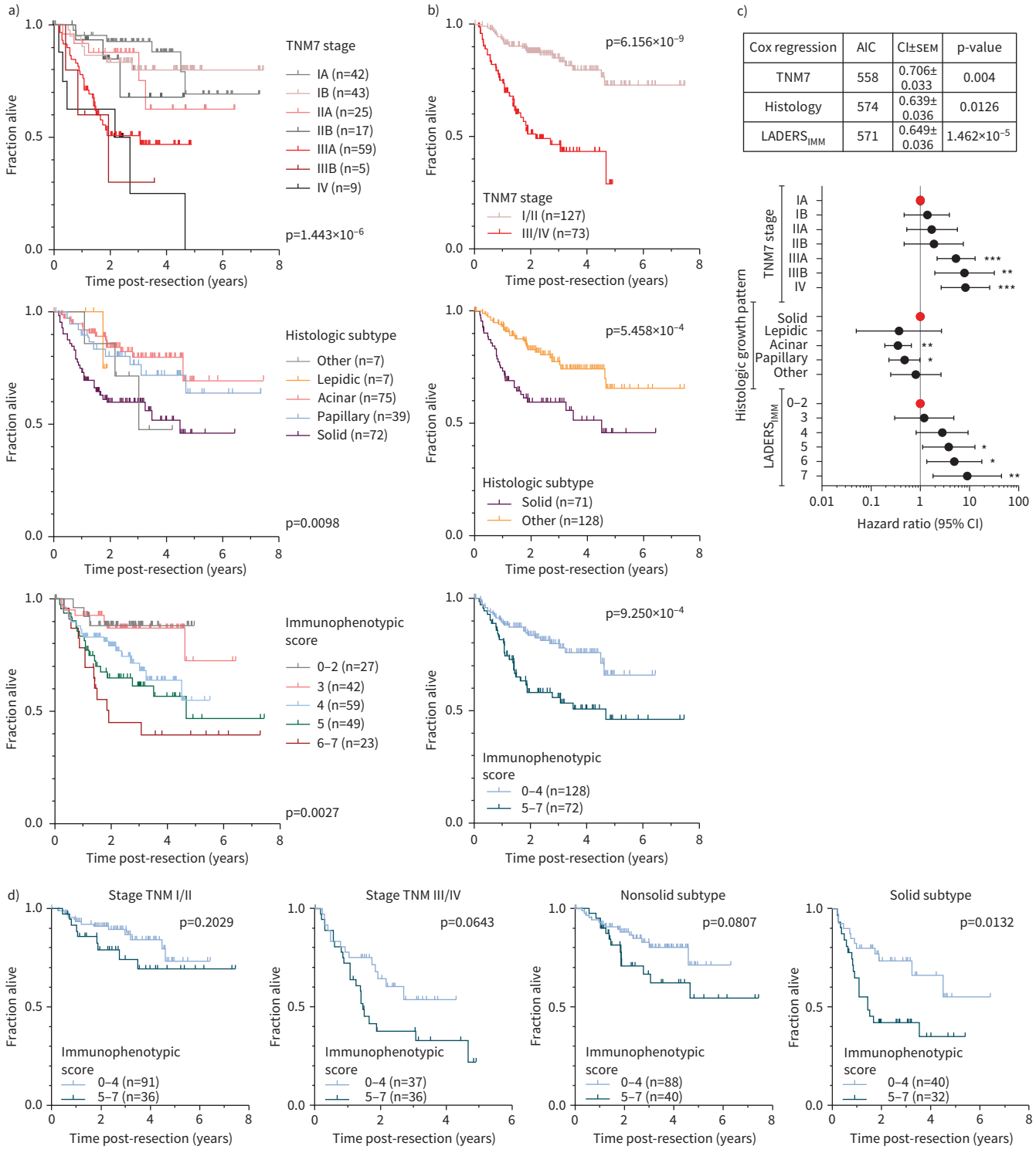

FIGURE 7 Lung adenocarcinoma (LUAD) immunophenotypic score complements International Association for the Study of Lung Cancer (IASLC) 7th edition tumor–node–metastasis (TNM7) stage and World Health Organization (WHO) histologic subtype. a, b) Overall survival of all patients stratified by TNM7 stage, histologic subtype and immunophenotypic score a) without and b) with category grouping shows that immunophenotypic score outperforms WHO histologic subtype and is outperformed by IASLC TNM7 stage. c) Results of Cox regression using TNM7 stage, histologic growth pattern and immunophenotypic score ($LADERS_{IMM}$) as inputs and overall survival as the target, showing Akaike Information Criterion (AIC), concordance index (CI)±SEM and overall log-rank p-value. *: p<0.05; **: p<0.01; ***: p<0.001, Cox regression. d) Overall survival of early- and advanced-stage patients with solid or other histologic growth patterns stratified by immunophenotype shows the increased value of the latter in advanced and solid disease. Data in a, b, d) are shown as patient numbers (n), Kaplan–Meier survival estimates (lines), censored observations (line marks) and log-rank p-values.

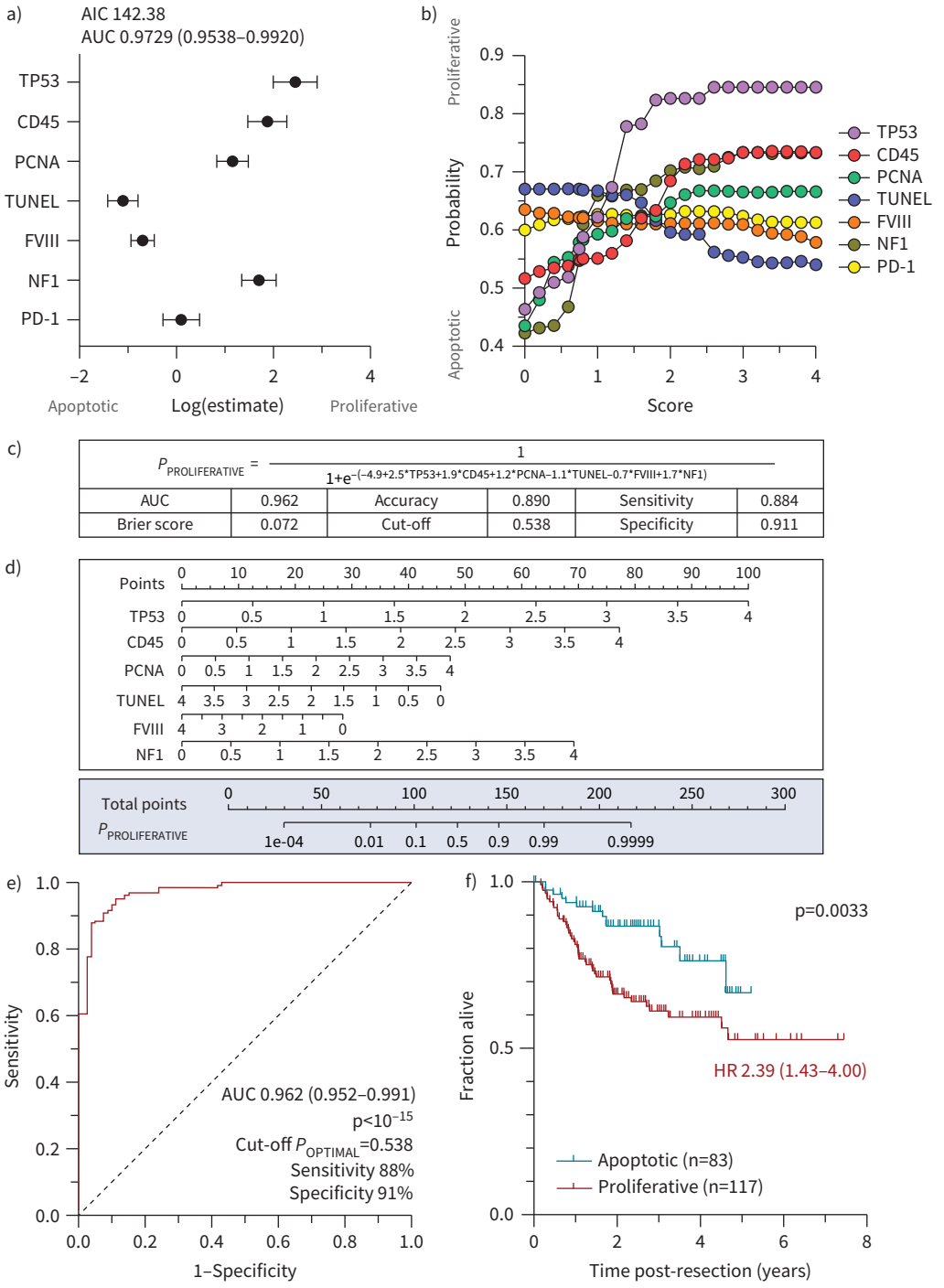

FIGURE 8 Cancer hallmarks predict lung adenocarcinoma (LUAD) phenotype and overall survival. a, b) Phenotype-predictive power of single cancer hallmarks using a) binary logistic regression and b) random forest analyses. Data in a) are shown as hazard ratios (95% CI), with area under the curve (AUC) (95% CI). c) Formula with its performance measures and d) nomogram for single-patient phenotype prediction by integral cancer hallmark expression. For examples of how to use the formula and nomogram, see the text and supplementary figure E5. e) Receiver operator characteristic of formula/nomogram in LUAD phenotype prediction. f) Overall survival of all patients stratified by formula-predicted phenotype. Data are shown as patient numbers (n), Kaplan–Meier survival estimates (lines), censored observations (line marks), hazard ratio (95% CI) and log-rank p-value. AIC: Akaike Information Criterion; TP53: tumour protein 53; CD45: cluster of differentiation 45; PCNA: proliferating cell nuclear antigen; TUNEL: terminal deoxynucleotidyl transferase dUTP nick-end labelling; FVIII: coagulation factor VIII; NF1: neurofibromatosis 1; PD-1: programmed cell death protein 1.

tumour areas and sections, as is done in routine pathology. Advanced statistics and machine learning identify two LUAD phenotypes solely detectable by cancer hallmarks and not any other clinical, pathological or molecular feature. Proliferative *versus* apoptotic LUAD phenotypes define overall survival to an extent comparable to IASLC TNM7 stage and WHO histologic pattern. A score, a formula and a nomogram to identify LUAD phenotypes and to predict overall survival are provided.

The hallmarks of cancer [24] have streamlined our perceptions of tumour biology, but their clinical impact is still under exploration. Phenotyping of bodily cancers by clinical-grade IHC provides pertinent guidance for treatment and prognosis, with the best example being breast cancer [23]. However, patients with early-stage resectable LUAD are still treated in a uniform fashion, grouped with other nonsmall cell lung tumours [2, 3], despite the fact that multiple studies have found that TNM stage-based overall survival prediction can be enhanced by many clinical, pathological and molecular variables [5–22]. We examined the possibility that LUAD patients might benefit from the current approach to breast cancer, which is treated and prognosticated based on validated molecular variables including IHC expression of marker of proliferation Ki-67 and oestrogen, progesterone and epidermal growth factor type 2 receptors [23]. We designed the present study in order to bridge this gap and investigated the value of IHC for cancer hallmarks in prediction of overall survival of LUAD patients. Indeed, we describe two LUAD phenotypes with markedly divergent overall survival. These proliferative $TP53^{hi}NF1^{hi}CD45^{hi}PCNA^{hi}$ and apoptotic $TUNEL^{hi}$ phenotypes can be discriminated immediately after surgery with 96% accuracy and can accurately predict overall survival. The findings can be readily tested in other cohorts using the score, formula and nomogram provided, and can potentially be incorporated in clinical trial design and/or patient management. For example, the findings can be used to prompt clinical and radiological vigilance for proliferative cases, but also to enhance clinical trial design for novel adjuvant therapies. To this end, we postulate that proliferative and apoptotic patients may exhibit differential therapeutic responses to adjuvant chemotherapy, targeted therapy and immunotherapy post-resection, based on their differential expression of PCNA (a proliferation marker), NF1 (a KRAS inhibitor) and CD45 (an inflammatory marker).

Our findings also trigger mechanistic hypotheses on LUAD evolution. In addition to histologic growth pattern and genomic landscape [5, 9], epidemiological data from atom bomb survivors [30] spark hypotheses on the existence of multiple molecular varieties of LUAD. The results presented here support such hypotheses: two phenotypes of LUAD are discovered solely based on expression of cancer hallmarks, which cannot be identified by driver mutation or any other clinicopathological feature. These phenotypes may be related to early initiating events such as environmental cause, replicative stress and/or cell of origin, or, more likely in our view, to late tumour diversity emanating from divergent mutagenic processes. Whatever the reason for their existence, we provide the means for characterisation of two molecular phenotypes of LUAD, which can be used for clinical management, trial design, as well as mechanistic studies on LUAD pathobiology. Notwithstanding the limitations of the present work, such as the use of an older TNM staging system and of a limited number of markers, future validation and clinical implementation of the proliferative and apoptotic phenotypes of LUAD described here may lead to therapeutic and research innovation.

Author contributions: M. Lindner, I. Koch and R.A. Hatz performed surgeries and procured data that were produced during surgeries. J. Behr performed clinical and physiological assessment. M.A.A. Pepe, M. Spella, I. Lilis, G. Ntaliarda, S.J. Behrend, G.A. Giotopoulou and A.C. Schamberger processed samples and provided important intellectual input. A-S. Lamort and W. Kujawa performed IHC. M.A.A. Pepe performed digital droplet PCR and analysed data; K. Somogyi and R. Sotillo analysed *ALK* fusions. A-S. Lamort, J.C. Kaiser and G.T. Stathopoulos designed and guided the study, analysed data, and wrote the manuscript. All authors critically reviewed and edited the paper for important intellectual content and approved the final submitted version. A-S. Lamort, J.C. Kaiser and G.T. Stathopoulos had full access to all the data of the study, had final responsibility for the decision to submit it for publication and are the guarantors of the study's integrity.

This study is registered at the German Clinical Trials Register with identifier number DRKS00012649.

Conflict of interest: The authors declare no potential conflicts of interest.

Support statement: This work was supported by European Research Council 2010 Starting Independent Investigator (260524) and 2015 Proof of Concept (679345) grants, the Graduate College (Graduiertenkolleg) 2338 of the German Research Society (Deutsche Forschungsgemeinschaft), the target validation project for pharmaceutical development ALTERNATIVE of the German Ministry for Education and Research (Bundesministerium für Bildung und Forschung), and a Translational Research Grant by the German Center for Lung Research (Deutsches Zentrum

für Lungenforschung) (all to G.T. Stathopoulos). The study sponsors had no role in study design, data collection, analysis and interpretation, and in writing and submitting the paper for publication. Funding information for this article has been deposited with the Crossref Funder Registry.

References

1 Global Burden of Disease Cancer Collaboration. Global, regional, and national cancer incidence, mortality, years of life lost, years lived with disability, and disability-adjusted life-years for 29 cancer groups, 1990 to 2017: a systematic analysis for the global burden of disease study. *JAMA Oncol* 2019; 5: 1749–1768.
2 Travis WD, Brambilla E, Nicholson AG, *et al.* The 2015 World Health Organization classification of lung tumors: impact of genetic, clinical and radiologic advances since the 2004 classification. *J Thorac Oncol* 2015; 10: 1243–1260.
3 Postmus PE, Kerr KM, Oudkerk M, *et al.* Early and locally advanced non-small-cell lung cancer (NSCLC): ESMO Clinical Practice Guidelines for diagnosis, treatment and follow-up. *Ann Oncol* 2017; 28: iv1–iv21.
4 Liang W, Zhang L, Jiang G, *et al.* Development and validation of a nomogram for predicting survival in patients with resected non-small-cell lung cancer. *J Clin Oncol* 2015; 33: 861–869.
5 Ujiie H, Kadota K, Chaft JE, *et al.* Solid predominant histologic subtype in resected stage I lung adenocarcinoma is an independent predictor of early, extrathoracic, multisite recurrence and of poor postrecurrence survival. *J Clin Oncol* 2015; 33: 2877–2884.
6 Duhig EE, Dettrick A, Godbolt DB, *et al.* Mitosis trumps T stage and proposed International Association for the Study of Lung Cancer/American Thoracic Society/European Respiratory Society classification for prognostic value in resected stage 1 lung adenocarcinoma. *J Thorac Oncol* 2015; 10: 673–681.
7 Klotz LV, Courty Y, Lindner M, *et al.* Comprehensive clinical profiling of the Gauting locoregional lung adenocarcinoma donors. *Cancer Med* 2019; 8: 1486–1499.
8 Warth A, Penzel R, Lindenmaier H, *et al. EGFR*, *KRAS*, *BRAF* and *ALK* gene alterations in lung adenocarcinomas: patient outcome, interplay with morphology and immunophenotype. *Eur Respir J* 2014; 43: 872–883.
9 Qian J, Zhao S, Zou Y, *et al.* Genomic underpinnings of tumor behavior in *in situ* and early lung adenocarcinoma. *Am J Respir Crit Care Med* 2019; 201: 697–706.
10 Izar B, Zhou H, Heist RS, *et al.* The prognostic impact of KRAS, its codon and amino acid specific mutations, on survival in resected stage I lung adenocarcinoma. *J Thorac Oncol* 2014; 9: 1363–1369.
11 Blackhall FH, Peters S, Bubendorf L, *et al.* Prevalence and clinical outcomes for patients with ALK-positive resected stage I to III adenocarcinoma: results from the European Thoracic Oncology Platform Lungscape Project. *J Clin Oncol* 2014; 32: 2780–2787.
12 Rizvi NA, Hellmann MD, Snyder A, *et al.* Cancer immunology. Mutational landscape determines sensitivity to PD-1 blockade in non-small cell lung cancer. *Science* 2015; 348: 124–128.
13 Cui Y, Fang W, Li C, *et al.* Development and validation of a novel signature to predict overall survival in "driver gene-negative" lung adenocarcinoma (LUAD): results of a multicenter study. *Clin Cancer Res* 2019; 25: 1546–1556.
14 Gentles AJ, Bratman SV, Lee LJ, *et al.* Integrating tumor and stromal gene expression signatures with clinical indices for survival stratification of early-stage non-small cell lung cancer. *J Natl Cancer Inst* 2015; 107: djv211.
15 Varghese C, Rajagopalan S, Karwoski RA, *et al.* Computed tomography-based Score Indicative of Lung Cancer Aggression (SILA) predicts the degree of histologic tissue invasion and patient survival in lung adenocarcinoma spectrum. *J Thorac Oncol* 2019; 14: 1419–1429.
16 Lee HY, Lee SW, Lee KS, *et al.* Role of CT and PET imaging in predicting tumor recurrence and survival in patients with lung adenocarcinoma: a comparison with the International Association for the Study of Lung Cancer/American Thoracic Society/European Respiratory Society Classification of Lung Adenocarcinoma. *J Thorac Oncol* 2015; 10: 1785–1794.
17 Takada K, Okamoto T, Shoji F, *et al.* Clinical significance of PD-L1 protein expression in surgically resected primary lung adenocarcinoma. *J Thorac Oncol* 2016; 11: 1879–1890.
18 Yanagawa N, Leduc C, Kohler D, *et al.* Loss of phosphatase and tensin homolog protein expression is an independent poor prognostic marker in lung adenocarcinoma. *J Thorac Oncol* 2012; 7: 1513–1521.
19 Cappuzzo F, Tallini G, Finocchiaro G, *et al.* Insulin-like growth factor receptor 1 (IGF1R) expression and survival in surgically resected non-small-cell lung cancer (NSCLC) patients. *Ann Oncol* 2010; 21: 562–567.
20 Kilvaer TK, Paulsen E-E, Khanehkenari MR, *et al.* The presence of intraepithelial $CD45RO^{+}$ cells in resected lymph nodes with metastases from NSCLC patients is an independent predictor of disease-specific survival. *Br J Cancer* 2016; 114: 1145–1151.
21 Ishida T, Kaneko S, Akazawa K, *et al.* Proliferating cell nuclear antigen expression and argyrophilic nucleolar organizer regions as factors influencing prognosis of surgically treated lung cancer patients. *Cancer Res* 1993; 53: 5000–5003.

22 Duarte IG, Bufkin BL, Pennington MF, *et al.* Angiogenesis as a predictor of survival after surgical resection for stage I non-small-cell lung cancer. *J Thorac CardiovascSurg* 1998; 115: 652–658.

23 Cardoso F, Kyriakides S, Ohno S, *et al.* Early breast cancer: ESMO Clinical Practice Guidelines for diagnosis, treatment and follow-up. *Ann Oncol* 2019; 30: 1194–1220.

24 Hanahan D, Weinberg RA. Hallmarks of cancer: the next generation. *Cell* 2011; 144: 646–674.

25 Groome PA, Bolejack V, Crowley JJ, *et al.* The IASLC Lung Cancer Staging Project: validation of the proposals for revision of the T, N, and M descriptors and consequent stage groupings in the forthcoming (seventh) edition of the TNM classification of malignant tumours. *J Thorac Oncol* 2007; 2: 694–705.

26 Kadota K, Nitadori JI, Sima CS, *et al.* Tumor spread through air spaces is an important pattern of invasion and impacts the frequency and location of recurrences after limited resection for small stage I lung adenocarcinomas. *J Thorac Oncol* 2015; 10: 806–814.

27 Lu S, Tan KS, Kadota K, *et al.* Spread through Air Spaces (STAS) is an independent predictor of recurrence and lung cancer-specific death in squamous cell carcinoma. *J Thorac Oncol* 2017; 12: 223–234.

28 Yagi Y, Aly RG, Tabata K, *et al.* Three-dimensional histologic, immunohistochemical, and multiplex immunofluorescence analyses of dynamic vessel co-option of spread through air spaces in lung adenocarcinoma. *J Thorac Oncol* 2020; 15: 589–600.

29 Campbell JD, Alexandrov A, Kim J, *et al.* Distinct patterns of somatic genome alterations in lung adenocarcinomas and squamous cell carcinomas. *Nat Genet* 2016; 48: 607–616.

30 Castelletti N, Kaiser JC, Simonetto C, *et al.* Risk of lung adenocarcinoma from smoking and radiation arises in distinct molecular pathways. *Carcinogenesis* 2019; 40: 1240–1250.